

Capacitance Improvement of Carbon Aerogels by the Immobilization of Polyoxometalates Nanoparticles

D.A. Baeza-Rostro and A.K. Cuentas-Gallegos*

Centro de Investigación en Energía, Universidad Nacional Autónoma de México
Privada Xochicalco S/N Col. Centro, AP 34, CP 62580 Temixco, Morelos, México

Received: September 10, 2012, Accepted: December 09, 2012, Available online: July 08, 2013

Abstract: A hybrid material based on the immobilization of $H_3PMo_{12}O_{40}$ polyoxometalate nanoparticles (POM) was obtained by using an activated carbon aerogel (ACPQ2-100) matrix, and was tested as a potential electrode material for a supercapacitor cell. A chemical activation with KOH was carried out in the carbon aerogel matrix (ACP-100), obtaining a greater BET surface area ($334\text{g}/\text{cm}^2$) and different electrochemical behavior (ACPQ2-100). Both matrices (ACP-100 and ACPQ2-100) were immersed in a 1.15mM POM solution in order to determine the role of the chemical activation procedure in the immobilization of POM nanoparticles. All materials were characterized by Attenuated Total Reflection (ATR) and nitrogen isotherms. For the electrochemical characterization, the synthesized materials were mixed with 10% of Teflon and 20% conducting carbon in weight ratio. Then, a film was made and a portion was pressed onto a stainless steel grid as current collector. Cyclic voltammetry in 3-electrode cells using a $0.5\text{ M H}_2\text{SO}_4$ electrolyte was used to determine the electrochemical performance. The chemical activation of the aerogel matrix with KOH was the key factor to immobilize and disperse the POM nanoparticles, which improved the capacitance behavior making this material suitable for its application as supercapacitor electrode material.

Keywords: carbon aerogels, polyoxometalates, supercapacitors, energy storage, hybrid materials

1. INTRODUCTION

Carbon aerogels are porous materials where their porosity and pore size distribution can be controlled by modifying the synthesis parameters. In these materials, the electric conductivity is higher than in typical activated carbons due to their continuous structure, which avoids the use of binders. In addition, the electrolyte can access almost all pores promoting high ionic conductivity. Therefore, carbon aerogels are promising electrode materials for supercapacitors [1].

From the literature, the electrochemical performance of carbon aerogels, among other carbonaceous materials, greatly depends on factors as specific surface area, pore size distribution, nature and concentration of surface functional groups [2]. These parameters can be tuned during the synthesis or the activation step. The activation of carbon materials proceeds via a chemical or a thermal route. In a thermal activation the surface area increases, probably due to mass loss in the material [3]. On the other hand, a chemical

route introduces some functional groups to the carbon matrix, aside from the increase of surface area in some cases.

Oxygen based functional groups are required to incorporate polyoxometalate particles (POM) onto a carbon matrix. Therefore, an activation process such as the chemical route with KOH can be carried out in order to obtain POM-based hybrid materials with carbon aerogels as the matrix. This KOH activation process increases the number of micro-meso pores and surface area as mentioned before, by creating pores in the carbon structure as well as incorporating functional groups (mostly OH groups) on the surface of the carbonaceous material.

POM particles are of great interest in energy storage applications due to their reversible multielectron redox reactions, and have been used as electrode materials for supercapacitors [4-6]. In the current study, an aerogel-type porous carbon material was prepared by using a molar ratio of resorcinol (R)/ formaldehyde (F) of 0.5 and a resorcinol (R)/ Na_2CO_3 catalyst (C) of 100, in order to obtain a high surface area aerogel matrix with pores in the range of 2-5nm. The novelty of this work is the incorporation of

*To whom correspondence should be addressed: Email: akcg@cie.unam.mx
Phone:

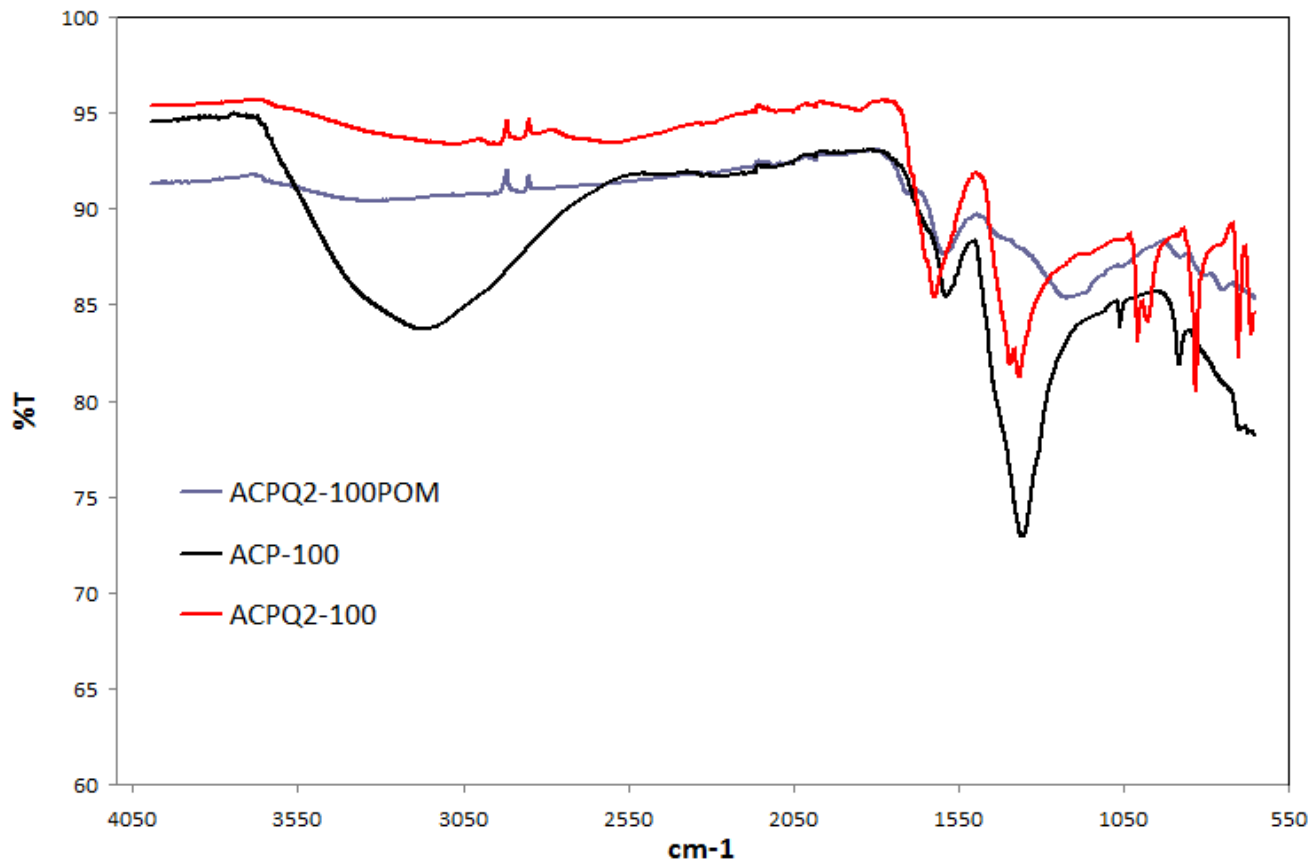


Figure 1. ATR spectra of ACP-100 (non-activated carbon aerogel matrix), ACPQ2-100 (activated aerogel), and ACPQ2-100/POM (hybrid material).

molecular oxides as polyoxometalates (POMs) onto the surface of chemically activated aerogel in order to improve capacitance.

2. EXPERIMENTAL

2.1. Synthesis of carbon aerogel and incorporation of POMs

Carbon aerogels (CAs) were synthesized using a R/F molar ratio of 0.5 and a molar ratio of R/C of 100. All reagents were used as purchased: Resorcinol (99% purity) from Reasol, formaldehyde from Fermont (37.4%; methanol stabilized), and sodium carbonate from Fermont (99.7% purity). All solutions were prepared with deionized water. First, all reagents in solution were stirred and placed on a cylindrical crystal jar in an oven at 85 °C for 96 hours to obtain the corresponding precursor gel (RF). In order to prepare this RF gel for the supercritical drying, a solvent exchange was carried out by adding acetone during three days by multiple replacement of residual water with fresh acetone. Subsequently the CO₂ supercritical drying was carried out by keeping the RF gel at 30 °C and under 7.4 MPa, using a SFT-100 equipment. This process was followed by a pyrolysis procedure during 30 min at 850 °C in order to obtain the carbon aerogel (ACP-100) with high surface area, as previously reported [7-9].

The chemical activation [10] of carbon aerogel (ACP-100) was performed by dissolving KOH in ethanol and mixing with ACP-

100 using a KOH/ ACP-100 mass ratio of 5/1. The mixture was dried at 110 °C and then heated in a tubular furnace at 850°C for 3 hours using a heating rate of 5°C/min. After the mixture cooled down to room temperature, the resultant materials were washed with a 10% HCl solution and deionized water. Finally, the material was dried at 110°C for 6h (ACPQ2-100).

The incorporation of POM particles was carried out in both carbon aerogel matrices (ACP-100 and ACPQ2-100), but no hybrid formation was obtained for the non-activated aerogel (ACP-100). Therefore, only the activated ACPQ2-100 matrix was used to obtain the hybrid material, and was performed by mixing 0.04 g of the activated carbon aerogel in a 1.7 mM H₃PMo₁₂O₄₀ (Fermont) solution in an ultrasound bath for 3h. The obtained suspension was filtered off and washed with a pH=2 sulfuric acid solution, and dried at 100°C for 1h.

Table 1. Surface area of carbon aerogel matrices and hybrids.

Sample	S _{BET} (m ² /g)
ACP-100	244
ACPQ2-100	334
ACPQ2-100/POM	274

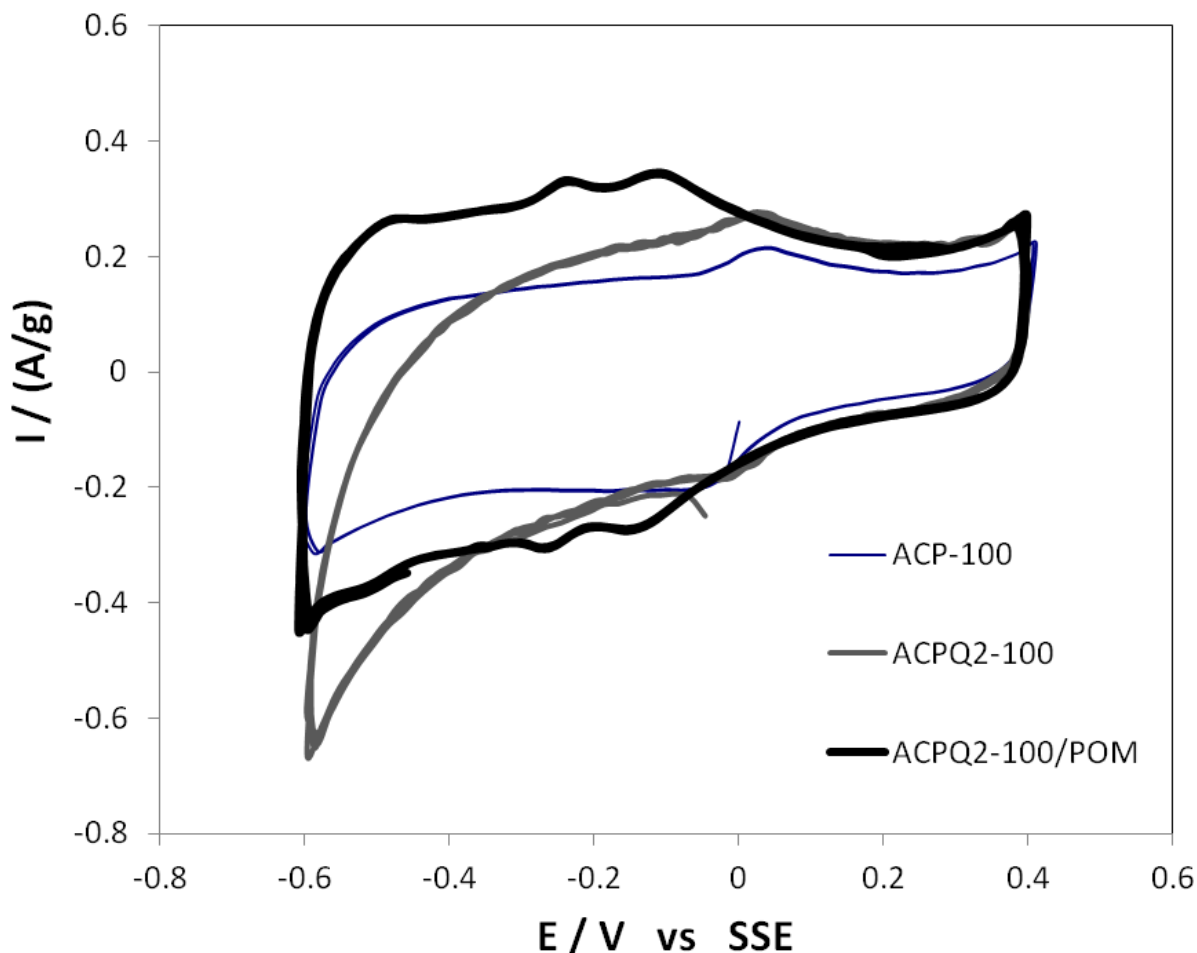


Figure 2. Cyclic voltammetry of the aerogel carbon matrices without activation (ACP-100) and activation with KOH (ACPQ2-100), and the hybrid material (ACPQ2-100/POM) at a scan rate of 10 mV/s in 0.5M H₂SO₄.

2.2. Structure and physical properties

Porosimetry measurements were carried out in a *Nova 1200e* (Quantachrome) equipment. The materials were degassed first at 120 °C under vacuum during 16 h, to remove all the adsorbed species before nitrogen adsorption and desorption isotherms were obtained. The surface area (S_{BET}) was calculated using BET (Brunauer-Emmett-Teller) equation in a relative pressure (P/P_0) from 0 to 0.3. Also, ATR analyses were performed directly over the sample to detect the different vibrational frequencies related with structural bonds from the different aerogel matrices, and to detect changes related with functional groups and/or incorporation of POM particles in the carbon aerogels.

2.3. Electrochemical characterization

Cyclic voltammetry (CV) technique was used to determine the electrochemical performance of the prepared electro-active materials, using an Arbin SuperCap model SCTS8 potentiostat. A 3-electrode cell was arranged using a 0.5 M H₂SO₄ solution as the electrolyte, a Pt gauze as the counter electrode, a sulfate saturated electrode (SSE) as the reference electrode, and our electroactive materials as the working electrode. All experiments were carried

out by first purging with nitrogen the electrolyte solution, to eliminate oxygen contributions. The working electrodes were prepared by mixing our grinded electro-active materials (CA and Hybrids) (60%) with a Teflon suspension (10%, ALDRICH), and conducting carbon (30%) in ethanol. This suspension was heated under continuous stirring until alcohol was evaporated (≈ 1.5 h) to yield a paste that was rolled to obtain a film. This film was cut in 1cm² squares and was pressed on to a stainless steel grid current collector (316L, chemically resistant to acidic media). The CV current is normalized with the electroactive material weight.

3. RESULTS AND DISCUSSION

All prepared carbon aerogel matrices were first characterized by nitrogen isotherms in order to calculate S_{BET} , and the results are presented in Table 1. The surface area of the carbon aerogel matrix (ACP-100) resulted in a value of 244 m²/g, which significantly increased, up to 334m²/g, when the activation process with KOH was carried out (ACPQ2-100). The incorporation of POM particles to obtain the hybrid material (ACPQ2-100/POM) with this activated matrix resulted in a decrease of the surface area (274m²/g), probably due to pore obstruction by POM particles. This phenome-

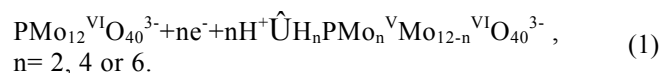
non has been previously observed in other carbon matrices used for POM immobilization [11-18], and incorporation of other functional groups like anthraquinone [19]. The mesoporosity of the materials was inferred from the hysteresis observed on the nitrogen isotherms (not shown here).

Figure 1 shows the ATR spectra obtained for the non-activated and activated carbon aerogel matrices, as well as the hybrid material. In general, the characteristic bands of the structure of these aerogel matrices are detected at 1557cm^{-1} and 1384cm^{-1} , and are related with the C=C stretching in the aromatic ring and with the connecting bridges $\text{CH}_2\text{-O-CH}_2$ formed during the gelation procedure (polycondensation). There are significant differences between both carbon aerogel matrices. One of these differences is the broad band around 3169cm^{-1} assigned to the vibrational stretching mode of the OH group. This stretching mode is observed with more intensity on the non-activated matrix (ACP-100) and could be related to a greater extent of physisorbed water molecules in the pores of the aerogel, or to residual byproducts formed during the synthesis. On the other hand, the activated matrix (ACPQ2-100) showed less intensity of this band probably due to the elimination of water and byproducts from the pores, and addition of OH functional groups. The addition of this functional group (OH) only on the activated matrix (ACPQ2-100) can be confirmed by the vibrational mode detected around 1000cm^{-1} , associated with C-O bonds. Nevertheless, we cannot rule out the presence of other type of ether (C-O-C) functional groups as epoxides on this activated matrix. In addition, around 880cm^{-1} a peak related with the graphitic structure formed during pyrolysis shows lower intensity in the activated matrix (ACPQ2-100), probably due to the introduction of defects by the previously detected functional groups. In order to confirm even more this hypothesis, at 770cm^{-1} and 820cm^{-1} intense peaks appeared only on this activated matrix (ACPQ2-100) and are related with alcohol and ether type functional groups, which are derived from the modification of the pristine aerogel by activation with KOH.

The introduction of POM nanoparticles to the activated matrix to obtain the hybrid material (ACPQ2-100POM) showed important modifications in its spectrum. Thus, a decrease or elimination of certain vibrational modes, such as the ones associated with $\text{CH}_2\text{-O-CH}_2$ (1384cm^{-1}) and functional groups (700cm^{-1} and 820cm^{-1}), confirms the interaction of POM with this activated matrix through oxygen based functional groups. Finally, the vibrational modes related with POM nanoparticles are detected at 1050cm^{-1} (P-O), 900cm^{-1} (Mo=O), and at 817cm^{-1} and 856cm^{-1} (Mo-O). The low intensity of these bands is probably due to its low concentration in the hybrid material.

Figure 2 shows the cyclic voltammograms obtained for the ACP-100 carbon aerogel, ACPQ2-100 activated matrix, and the correspondent ACPQ2-100/POM hybrid material. The most relevant

difference between the voltammograms of these samples is their profile change. The bare ACP-100 carbon aerogel shows a rectangular profile typical of a capacitive behavior, but the current range is the smallest and is revealed in the low capacitance value (table 2). The activated carbon aerogel (ACPQ2-100) shows a voltammogram profile deviated in the negative voltage range from the typical rectangular shape characteristic of the capacitive behavior, which indicates a resistive nature in this material probably due to the presence of functional groups. Nevertheless, the current range increased considerably in comparison with the pristine matrix, making the chemical activation with KOH effective to improve electrochemical performance. On the other hand, the hybrid material voltammogram shows a more evident rectangular profile, confirming its capacitive behavior and less resistive contribution compared with its matrix (ACPQ2-100). In addition, three redox pairs at $-0.13\text{V}/-0.1\text{V}$, $-0.27\text{V}/-0.24\text{V}$, and at $-0.5\text{V}/-0.47\text{V}$ are detected and correspond to the typical six electron transfer of POM particles confirming its presence [23]. In equation 1 we show these multiple reversible redox reactions.



We must point out that in comparison with previous publications from our group [17,18] the POM content in this hybrid material is low, and can be deduced from the area of the redox peaks. These results suggest that functional groups generated during the chemical activation are responsible for the resistive nature in the activated matrix (ACPQ2-100), since in the hybrid material this phenomenon is considerably reduced probably due to the bonding of these groups with POM particles, in good agreement with ATR results.

From these voltammograms, capacitance values were evaluated by applying eq. (2).

$$C = I \left(\frac{t}{\Delta V} \right) \quad (2)$$

where C is the capacitance I is the applied current, t is the discharge time, and ΔV is the voltage window as a function of the discharge process. Capacitance values for all samples are reported in Table 2, and a capacitance improvement from 59F/g for the pristine carbon aerogel (ACP-100) to 78F/g for the bare activated matrix (ACPQ2-100), were improved to a higher value of 84F/g for the hybrid material. This capacitance improvement without any doubt, is due to the incorporation of POM nanoparticles interacting with functional groups from the activated CA matrix (ACPQ2-100).

4. CONCLUSIONS

Incorporation of POM particles on to the surface of activated carbon aerogel matrix (ACPQ2-100) was confirmed by the decrease in BET surface area, from $334\text{ m}^2/\text{g}$ to $274\text{ m}^2/\text{g}$ due to pore obstruction, by the presence of vibrational modes characteristic of POM in the ATR spectrum, and by the appearance of the three typical reversible redox processes of POM. ACPQ2-100/POM hybrid material showed an improved electrochemical behavior, with a rectangular shape voltammogram profile indicative of a

Table 2. Capacitance Values of all carbon aerogel samples and hybrid material.

Sample	Capacitance (F/g)
ACP-100	59
ACPQ2-100	78
ACPQ2-100/POM	94

capacitive behavior with a smaller resistive nature compared to its activated matrix (ACPQ2-100), aside from the faradic contribution of the three redox process of the POM particles. These results show a clear improvement of the capacitance value from 59F/g for the pristine carbon aerogel to 94F/g for the hybrid material.

5. ACKNOWLEDGEMENTS

We acknowledge the technical work of Patricia Altuzar-Coello and the financial support granted from CONACYT Basic Science Project 154259 and PAPIIT Project IN105410.

REFERENCES

- [1] H. Pröbstle, R. Saliger, J. Fricke, K.K. Unger, G. Kreysa, J.P. Baselt, *Studies in Surface Science and Catalysis*, 128, 371 (2000).
- [2] Junbing Wang, *Journal of Power Sources*, 185, 589 (2008).
- [3] R. Saliger, U. Fisher, C. Herta, J. Fricke, *Journal of Non-Crystalline Solids*, 225, 81 (1998).
- [4] P. Gómez-Romero, K. Cuentas-Gallegos, M. Lira-Cantú and N. Casañ-Pastor, *Journal of Materials Science*, 40, 1423 (2005).
- [5] A.K. Cuentas-Gallegos, M. Gonzales-Toledo and M.E. Rincón, *Revista Mexicana de Física*, 53, 91 (2007).
- [6] P. Gómez-Romero, M. Chojak, K. Cuentas-Gallegos, J.A. Asensio, P.J. Kulesza, N. Casañ-Pastor, M. Lira-Cantú, *Electrochemistry Communications*, 5, 149 (2003).
- [7] M.H. Mirzaeian, *Journal of Materials Science*, 44, 2705 (2009).
- [8] Tamon, H. Ishizaka, T. Araki and M. Okazaki. *Carbon*, 36, 1257 (1998).
- [9] R.W. Pekala, J.C. Farmer, C.T. Alviso, T.D. Tran, S.T. Mayer, J.M. Miller and B. Dunn, *Journal of Non-Crystalline Solids*, 225, 74 (1998).
- [10] Xianhua Zeng, *Electrochimica Acta*, 53, 5711 (2008).
- [11] A.K. Cuentas-Gallegos, S. Peñaloza-Jiménez, D.A. Baeza-Rostro, A. Germán-García, *Journal of New Materials for Electrochemical Systems*, 13, 369. (2010).
- [12] R.D. Gall, C.L. Hill, J.E. Walker, *Chemistry of Materials*, 8, 2523 (1996).
- [13] J. Alcañiz-Monge, G. Trautwein, S. Parres-Esclapez, J.A. Maciá-Argulló, *Microporous and Mesoporous Materials*, 115, 440 (2008).
- [14] Mukai S.R., *Applied Catalysis A: General*, 256, 99 (2003).
- [15] Ghetti P., Ricca L., Luciana A., *Fuel*, 75, 565 (1996).
- [16] Pastor-Villegas J.J., Gómez-Serrano V., Durán-Valle C.J., Higes-Rolando F.J., *Journal of Analytical and Applied Pyrolysis*, 50, 1 (1999).
- [17] A.K. Cuentas-Gallegos, A. Zamudio-Flores, M. Casas-Cabanas, *Journal of Nano Research*, 14, 11 (2011).
- [18] A.K. Cuentas-Gallegos, M. Miranda-Hernández, A. Vargas-Ocampo, *Electrochimica Acta*, 54, 4378 (2009).
- [19] (a) G. Pognon, T. Brousse, D. Bélanger, *Carbon*, 49, 1340 (2011). (b) G. Pognon, T. Brousse, L. Demarconnay, D. Bélanger, *Journal of Power Sources*, 196, 4117 (2011).
- [20] Jun Li, Xianyou Wang, Qinghua Huang, Sergio Gamboa, P.J. Sebastian, *Journal of Power Sources*, 158, 784 (2006).
- [21] C. Liang, G. Sha, S. Guo, *Journal of Non-Crystalline Solids*, 271, 167 (2000).
- [22] Conley R.T., *Espectroscopía Infrarroja.*, Madrid Ed. ALHAMBRA, S.A. 1979.
- [23] A.K. Cuentas-Gallegos, M. Lira-Cantu, N. Casañ-Pastor and P. Gómez-Romero, *Advanced Functional Materials*, 15, 1125 (2005).